

# PROJECT REPORT 2000-11

sustainable  
forest  
management  
network

réseau  
sur la  
gestion durable  
des forêts



## Computational Fluid Dynamics Modelling of Aerated Stabilization Basins



For copies of this or other SFM publications contact:

Sustainable Forest Management Network  
G208 Biological Sciences Building  
University of Alberta  
Edmonton, Alberta, T6G 2E9  
Ph: (780) 492 6659  
Fax: (780) 492 8160  
<http://www.ualberta.ca/sfm/>

ISBN 1-55261-069-1

# **Computational Fluid Dynamics Modelling of Aerated Stabilization Basins**

**SFM Network Project:  
Development of Simulators for Biological Treatment Systems**

by

**R. Wayne Jenkinson, Eric R. Hall and Gregory A. Lawrence**

**Department of Civil Engineering and Pulp and Paper Centre  
The University of British Columbia, Vancouver, B.C.**

**July 2000**

## ABSTRACT

This study endeavored to apply computational fluid dynamics (CFD) techniques to aerated stabilization basins (ASBs) on a laboratory scale. A laboratory study was set up to assess the hydraulic impacts of a small-scale mechanical surface aerator in a still-water tank. A small surface mechanical aerator was built that would circulate from 0.5 to 4 L/sec. The aerator was employed in a tank and the velocity patterns imparted by the aerator were measured using an acoustic Doppler velocimeter (ADV). The velocity profiles were converted into dispersion parameters for use in a CFD model. A local turbulent time scale method was used to determine an approximate dispersion value as a function of distance from the aerator. The analysis examined different aerator power settings under otherwise identical conditions. Three successful runs were completed. The chaotic patterns within the tank induced by the aerator, produced turbulent structures that were not easily resolved using a time averaged statistical turbulence approach.

Tracer studies were performed in the same basin, modified to provide a flow-through environment. The studies were performed with and without aeration and at different flow-through rates. Tracer study results were examined and some of the typical parameters used in the literature were extracted for comparative analysis. The trends were surprising as the dimensionless axial dispersion number was inversely related to the degree of mixing applied.

A two-dimensional computational fluid dynamics (CFD) model was employed to model the fluid flow within the basin without aeration using a commercial package, FLUENT. The modeling results were compared with depth-averaged ADV velocity measurements taken within the basin. Many CFD modeling parameters were varied, including grid size and structure, turbulence modeling and boundary condition modeling. The model compared well with the ADV data.

The results from the FLUENT modeling were applied to a second CFD model that solved the solute transport equations over a structured grid. The solute transport modeling only examined the transport equations with uniform dispersion over the basin and, although it was the original intent, no attempts were made to model aeration at this stage. The overall shape of the modeled tracer curves compared favourably to the tracer study data obtained in the lab.

## **ACKNOWLEDGEMENTS**

The authors would like to thank the Natural Sciences and Engineering Research Council of Canada, the NSERC/COFI Industrial Research Chair in Forest Products Waste Management and the Sustainable Forest Management Network of Centres of Excellence, for their financial support.

## INTRODUCTION

The aerated stabilization basin (ASB) is the most common secondary wastewater treatment system utilized by the forest products industry. ASBs are partially mixed, aerated reactors that degrade wastes biologically prior to discharge into the environment. These systems are characterized by hydraulic retention times of 3 - 10 days, are 1 - 5 m deep and occupy hectares of surface area. Structurally, these systems are very simple, being essentially shallow, lined, flow-through ponds, usually with mechanical surface aerators included to provide the necessary oxygen and mixing required for waste stabilization.

It is known that the performance of ASBs and related systems is highly dependent on the flow conditions (Nameche and Vasel 1998). The modeling of substrate decay typically uses an exponential decay equation based on the time the substrate spends in the reactor. The efficiency of the hydraulics of a system will have a direct impact on the amount of time the substrate will spend in the system, on average, and therefore will have a direct effect on the system performance. A variety of techniques have been developed to examine the hydraulics of reactors and specifically ASBs and waste stabilization ponds, but until recently, these were very simplistic mathematical models that attempted to model the reactor by simplifying the reactor to a representative model that reproduces the bulk fluid mixing response. Recently, more innovative techniques have arisen in the field of computational fluid dynamics (CFD) that examine the more detailed flow fields within reactors, allowing the hydraulic performance and mixing characteristics of the reactor to be extracted from the CFD solution. Some effort has been made to apply the CFD techniques to the problems of waste stabilization ponds and aerated stabilization basins. However, none have considered directly the hydraulic impacts of the aerators themselves. Literature unrelated to CFD analysis has shown the importance of aeration in determining the degree of mixing in an ASB (Nameche and Vasel 1998). This study attempted to examine the impacts of aerators on ASBs, using a laboratory scale apparatus. When the apparatus was constructed, several factors that ordinarily may have an impact on ASBs, were effectively neglected in this study. Only a single aerator was included in the study, so the effects of multiple aerators or aerator interaction were not addressed. The aerator was always placed in the center of the tank, so that the effects of aerator placement were not addressed.

The study did address several issues related to the inclusion of aeration in reactor tanks. The flow calibration of a model aerator was examined. The impact on the velocity fields in the surrounding waters of an aerator at various power settings was examined. The change in residence time distribution (RTD) was examined in a flow-through tank, with and without

aeration, and the matching of flow field velocity measurements and RTD curves from CFD modeling to laboratory data was undertaken.

The itemized list of objectives was as follows:

1. To determine, using a laboratory scale apparatus, the velocity and turbulence profiles induced around a small-scale surface mechanical aerator, whereby a determination of mixing imparted by the aerator could be calculated as a function of distance from the aerator and aerator flow rate. Detailed knowledge of flow patterns is critical for the incorporation of an aerator model into a CFD routine.
2. To conduct a series of tracer studies to provide detailed bulk-mixing relationships between degrees of mixing in the basin and the shape of the residence time distribution curves; and
3. To produce a two-dimensional CFD model that incorporates the mixing influence of a surface mechanical aerator and accurately reproduces the RTD curves of the of a basin with and without mixing.

Further details on this study are available in Jenkinson (2000).

## AERATOR AND BASIN CONSTRUCTION

A laboratory-scale tank and an aerator were designed and built to test hydraulic impacts of an aerator on its surrounding water. The aerator was designed to be similar to many of the types of surface mechanical aerators used by the wastewater treatment industry. A scale drawing of the aerator built for this study is provided in Figure 1. The flow through the aerator was driven by a 3.8 cm diameter impeller sleeved by a 20 cm diameter draught tube. The draught tube was removable and although several lengths of tube were available, only the 20 cm draught tube was employed in this study. The water drawn up through the tube was sprayed laterally by a splash plate. A 90-Watt DC motor, the power to which was controlled by a 10-point rheostat, powered the propeller. The entire apparatus was supported by stilts and rested on the floor of the study basin.

The aerator was designed so that many of the important dimensions could be adjusted. The position of the motor could be moved relative to the splash plate, allowing for independent positioning of the propeller (shown as dimension "B" in Figure 1). The position of the draught tube could be moved up or down relative to the splash plate (dimension "C") and the entire apparatus could be moved up and down along the main support stilts allowing for accurate positioning within the water column (dimension "A"). The width and height dimensions of the

aerator are shown in Figure 1 to illustrate the size of the aerator. It had a base diameter of 38.1 cm (15 inches) and a vertical support rod height of 83.8 cm (33 inches).

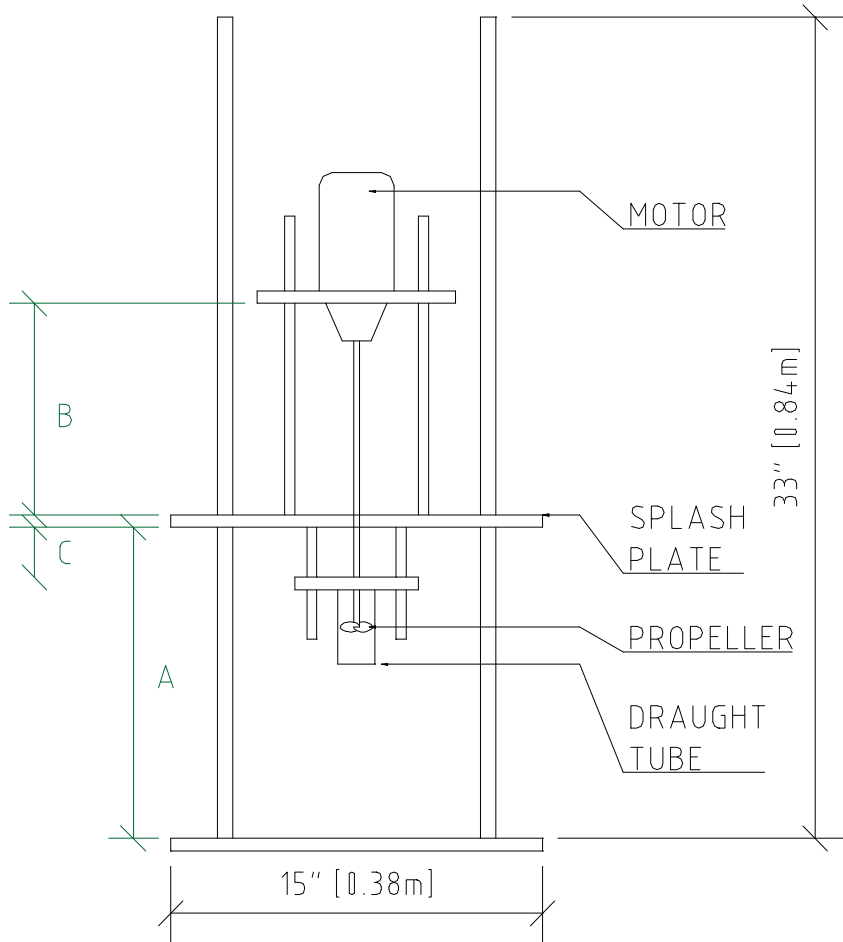


Figure 1: Model aerator schematic.

The basin in which the testing of the aerator took place was 3.7 m wide, 5.5 m long and 0.61 m deep. The basin could be configured for still water aerator studies (i.e. no ambient flow field), or flow through conditions. The basin was filled with water from the Vancouver water distribution network, and was seeded with silica particles of approximately 8  $\mu\text{m}$  in diameter to increase the acoustic response of the velocity measurement device, described below. Approximately 2000 mL of the silica particles were used to seed the basin when full, but the amounts added were not precise and silica was added only as required. Figure 2 shows a construction drawing of the basin, including the support struts along the sides.

The rationale in determining an appropriate size for the test basin and aeration device involved some comparison of aerator flow rates to reactor volume ratios and attempting to size the aerator accordingly for this study. The size of the basin was essentially fixed by the available space in the laboratory at approximately 7.0 m<sup>3</sup> (at a water depth of 0.42 cm). The aerator was designed to produce a comparable flow ratio to that observed in the field. Communications with an aerator manufacturer (Aqua-Aerobic Systems Inc.) provided some approximate flow rates for 75 HP surface mechanical aerators. These aerators are employed at an ASB in Grande Prairie, Alberta. An additional study provided in the literature (Aqua-Aerobic 1998) cited a reactor with identical mechanical aerators in a mill aerated lagoon system in Boyle, Alberta. Table 1 below illustrates the approximate Volume to Flow ratios.

Table 1: Existing mill volume to flow ratios

<b>Mill</b>	<b>Volume (m<sup>3</sup>)</b>	<b>Number of Aerators</b>	<b>Volume / Flow Ratio (hrs)</b>	<b>Target Model Aerator Flow Rate (L/sec)</b>
Grande Prairie, AB	836 000	30	6.9	0.30
Boyle, AB	100 000	21	1.2	1.9

Assuming that these were fairly typical values of aerator flow density, the aerator designed for the present study should have an approximate flow range of 0.3 L/sec to 1.9 L/sec. It was difficult to determine the flow of the aerator prior to actual construction but with the knowledge of the pitch, and diameter of the impeller blade and approximate rotations per minute of the motor known the flow rate of the aerator could be approximated. This was done by assuming the effect of gravity was small and that the water would be conducted through the draught tube very much like a solid, with the velocity equal to the rotational speed multiplied by the blade pitch. Allowances were made for efficiencies of 70% to 90% to provide a reasonable range of flow rates. The actual flow range after construction was higher than the proposed range with a lower limit of about 0.5 L/sec and an upper limit of about 4.0 L/sec. However, this higher flow rate was not seen as a real difficulty, as the scaling shown in Table 1 did not consider the increased contribution of viscosity at the lower scales, therefore a higher degree of mixing would be desirable when linearly relating the flow scales. For mixing, one would like to find similarity with Reynolds numbers between the two systems in the surrounding waters, but with the flow fields around the full-scale aerators uninvestigated and the issues of splashing complicated the similarity analysis.

It was decided that the aerator, once built with a reasonable flow and mixing rate, would exhibit a degree of mixing that could be measured and hopefully modeled. Success in modeling

of the aerator in this tank would not necessarily scale directly to a full scale apparatus, but the techniques used in modeling this system could be applied to a full scale modeling endeavor.

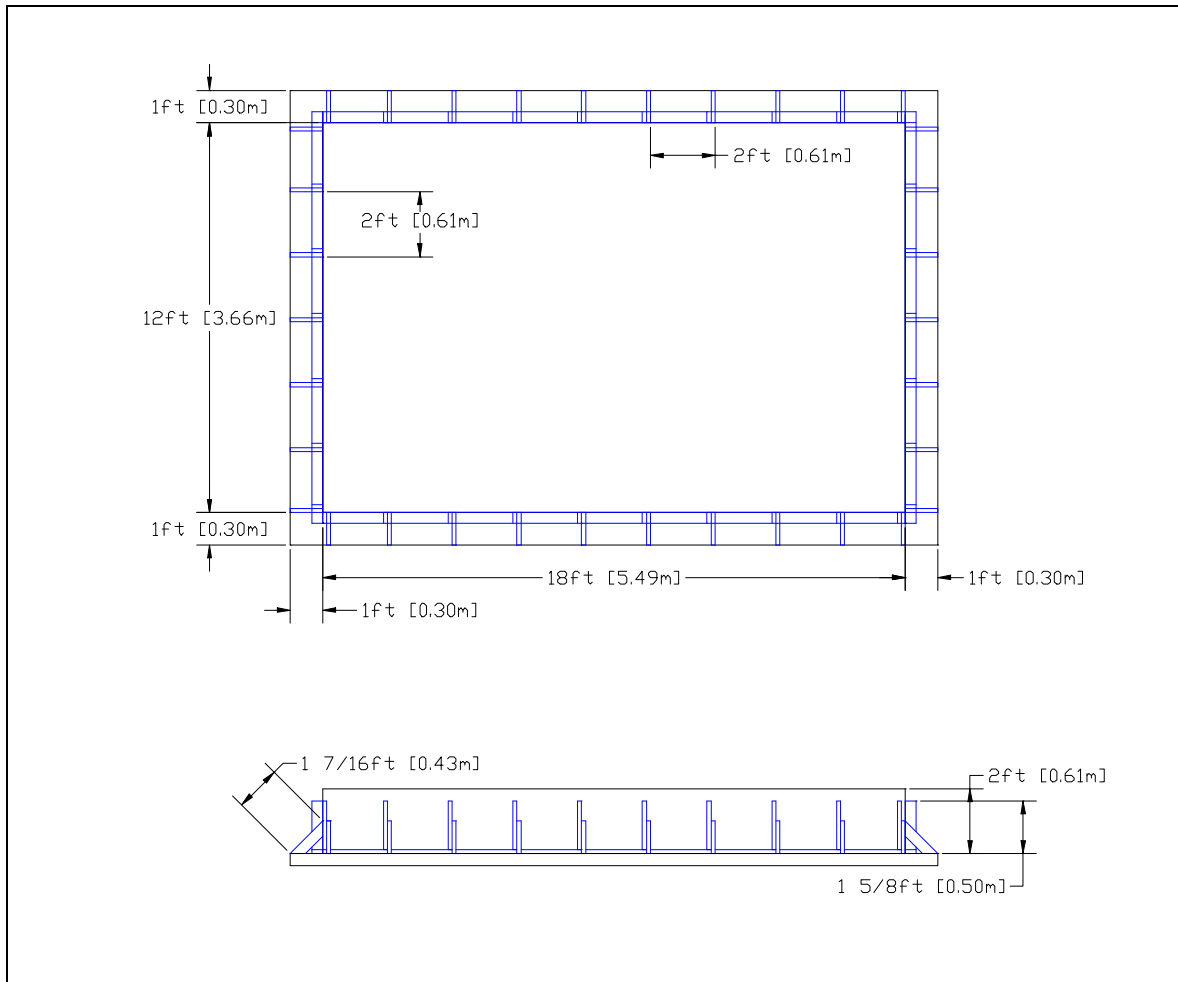


Figure 2: Basin schematic.

### Still-Basin aerator testing

In order to examine the impacts of the aerator on the surrounding water body, the aerator was placed into the tank at the center and operated in water without any bulk flow. Prior to data collection, the aerator was activated and allowed to run for 30 to 40 minutes to allow the basin to reach steady state conditions. The ADV probe was set so that the sample volume was along the normal line that ran perpendicular to the cross bridge and the center of the aerator. Care was taken to ensure that the ADV was properly oriented (i.e. the axes of the instrument corresponded to the three principal directions of the basin). Velocity measurements were obtained by the ADV at a frequency of 25 Hz for a specified period of time. Velocity measurements were made in a grid-like pattern in a plane extending radially from the aerator and over the vertical depth of the water. Figure 3 illustrates the location of the sampling plane with respect to the basin and the

aerator. Samples were taken at 20 cm increments horizontally from the aerator from 50 cm distance to 190 cm distance and at 5 cm increments vertically from 4 cm from the surface of the water along the depth to a minimum depth of 7 cm. These limits on measurement were constrained by the physical shape of the tank and the aerator. A distance 50 cm from the aerator was only 30 cm from the edge of the aerator itself just beyond the splash zone. The ADV was found to not provide accurate velocity measurements when closer than 3 cm to the water surface or the basin floor. Velocity data were collected at each location for 7 minutes to ensure that the larger scale velocity fluctuations were captured in the sample time series.

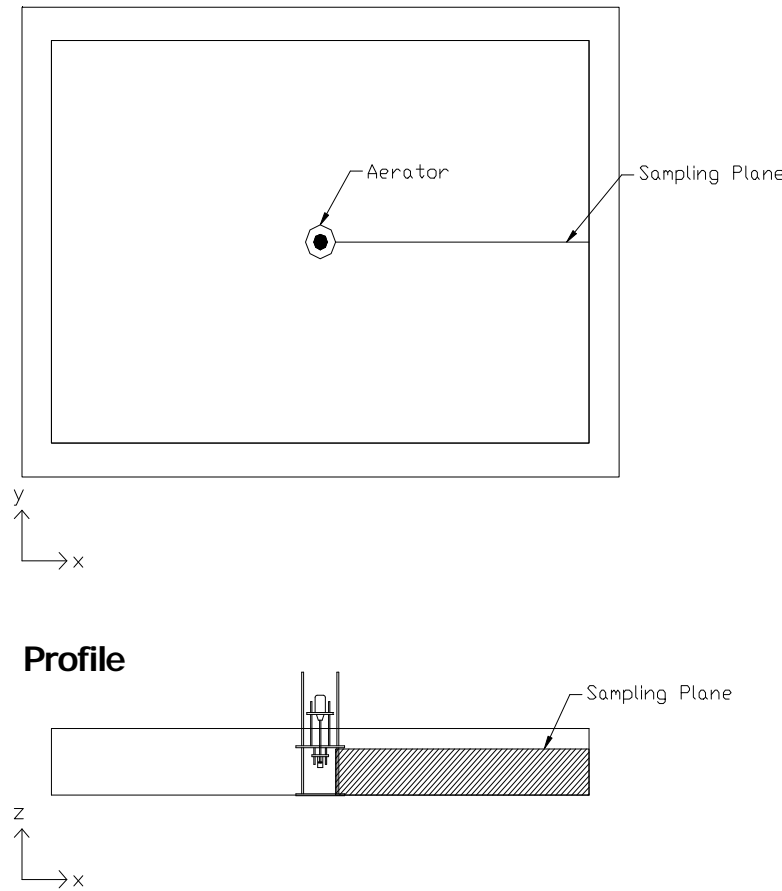


Figure 3: Velocity measurement sampling plane.

## VELOCITY PROFILE RESULTS

### Velocity profiles under no-flow conditions

Figure 4 shows u-velocity (velocity in x-direction) plots at various distances from the center of aerator (x). The plots show the in-plane horizontal velocity at the points measured against a dimensionless depth which is the height of the measuring point over the total water depth. The

**P=7; Q=3.1 L/sec**

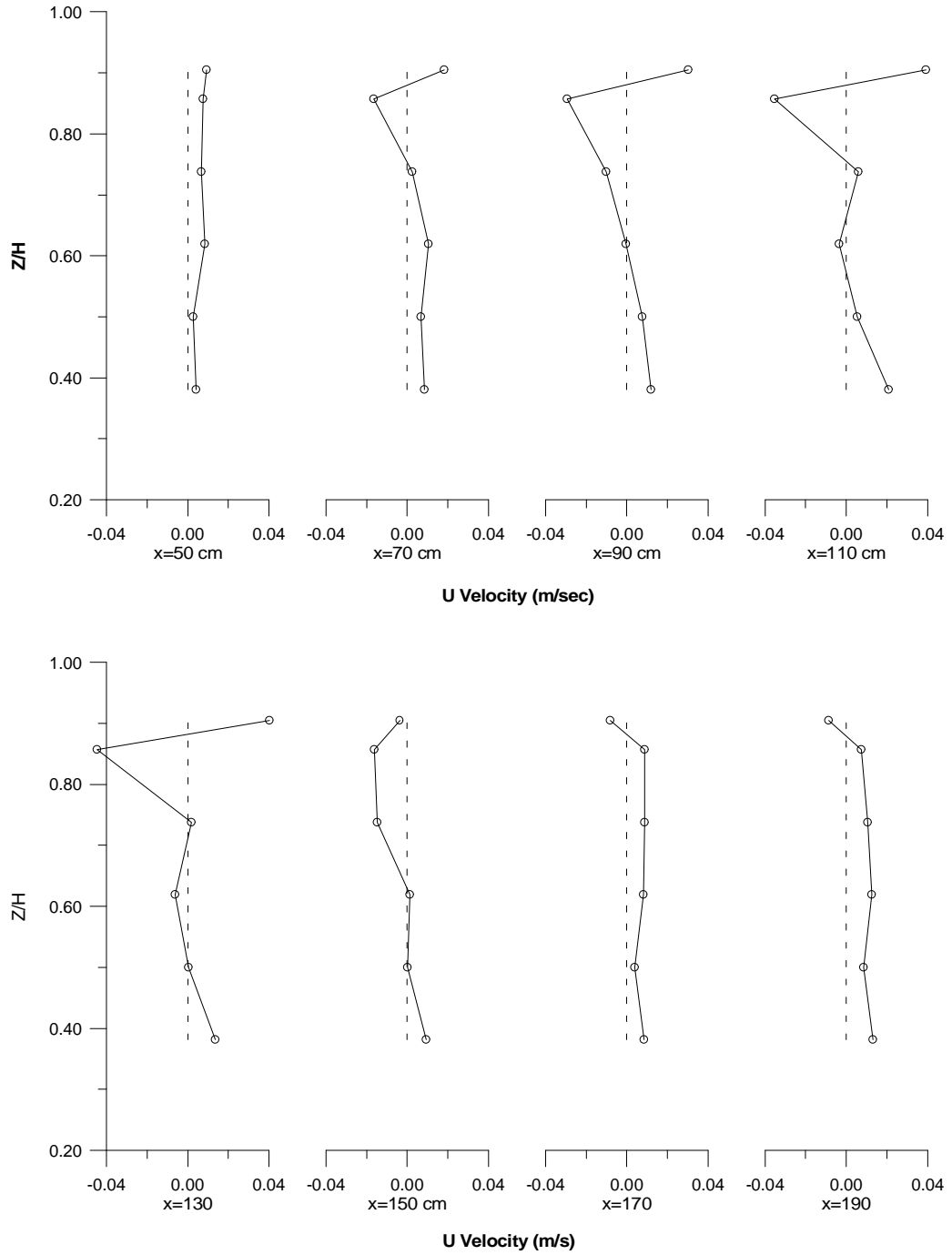


Figure 4: U velocity profiles - power 7,  $Q=3.1 \text{ L/sec}$ .

water depth was 42 cm in all runs and aerator flow was set to 3.1 L/sec. A velocity field at the surface moving away from the aerator can be seen with a recirculation zone of some shape beneath it. It can be seen that at some positions, all measured velocities move in a single

direction over the depth (e.g.  $P=7$  at distance of 50 cm). This observation seems to indicate that a flow mass-balance can not be resolved in the sampling plane using the sampling procedure employed. This could have been due to the presence of three-dimensional flows, inadequate sampling duration or too coarse a spatial sampling resolution. The inability to resolve flow fields may also have been a result of chaotic mixing patterns with the flow fields changing as the sampling progressed.

Figure 5 shows a sample of turbulence data calculated from the same data presented in Figure 4. This data show that the turbulence is predominantly a surface phenomenon and that the circulation zone matches the horizontal extent of the turbulent plume.

A relationship between the size of the mixing zone and the aerator flow rate could not be clearly observed. Also, the intensity of turbulence in the flow field was very highly dependent on the flow through the aerator as seen in Figure 5. The profiles themselves seem to generally match those presented by NCASI (1971), in that the highest velocities are evidenced at the surface with an velocity magnitude decay with increasing distance and a bottom recirculation zone.

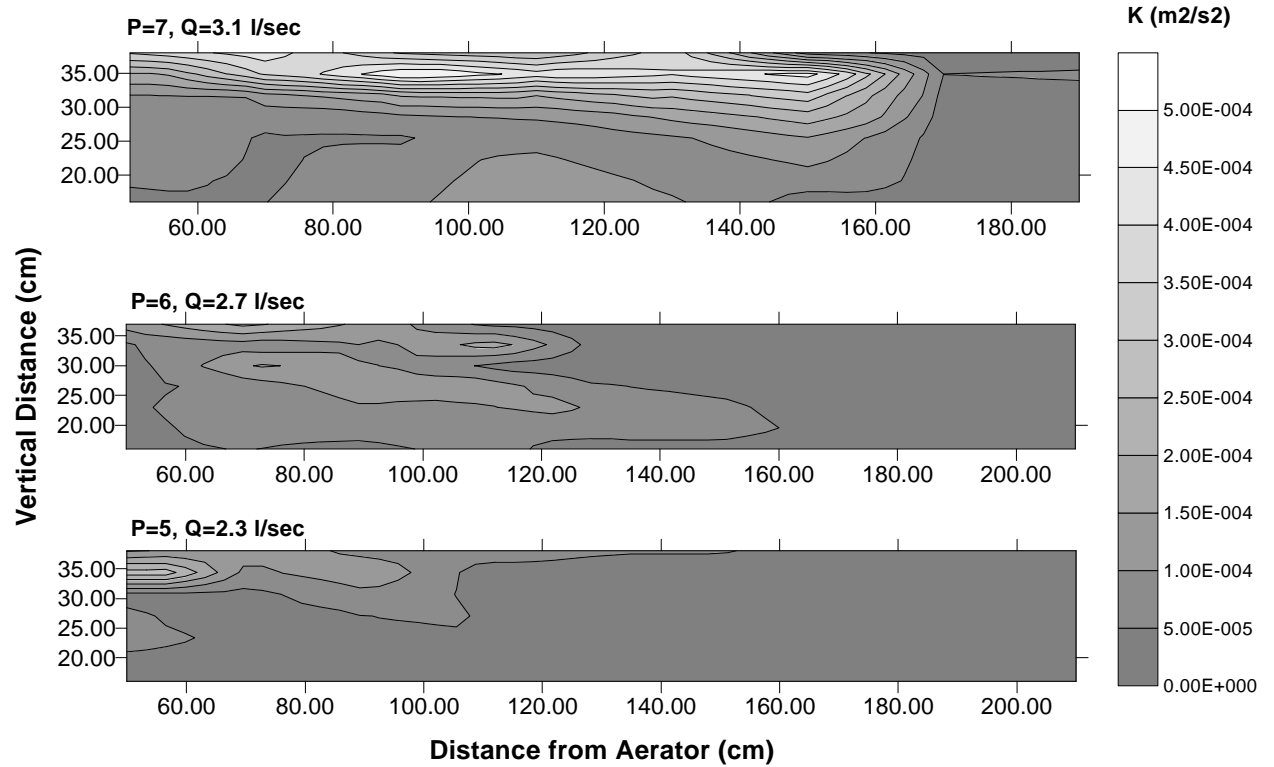


Figure 5: Turbulent kinetic energy ( $k$ ) profiles.

### **Depth-integrated trends**

In an effort to incorporate the aerator data into a depth-averaged 2D CFD model, the parameters of interest were examined by integrating over the depth and examining the trends. An attempt was made to approximate the dispersion number as a function of distance from the aerator. The technique used was one outlined by Fisher et al. (1979) for dispersion in isotropic turbulence. The technique requires the calculation of the turbulent time scale for the turbulent covariance in each of the principle directions.

Prior to depth-averaging the values of the turbulent time scale and dispersion, the average of the three directional components was determined. The averaging of the components would provide a parameter of use in CFD modeling. It is this average value that was, in turn, averaged over the depth of the water column to produce the plots that follow in Figure 6. The results were difficult to interpret. The turbulent kinetic energy depth-averaged profiles seem to make reasonable sense, with the highest value profiles being associated with the greatest flow rate through the aerator and with the profile being generally higher near the aerator, than away from it.

The turbulence time scale data are less straightforward. The 2.7 and 2.3 L/sec profiles show interesting trends with gradual increases in time step with a sudden drop and a further gradual increase. The higher velocity, 3.1 L/sec profile exhibits a much lower average turbulence time scale with a markedly different profile shape.

The dispersion number profiles are products of the turbulent time scales and turbulent correlation's and as a result, reflect the differences discussed in the previous two plots. As seen in Figure 6, the dispersion profile intensities are not clearly related to the aerator flow rate by this method.

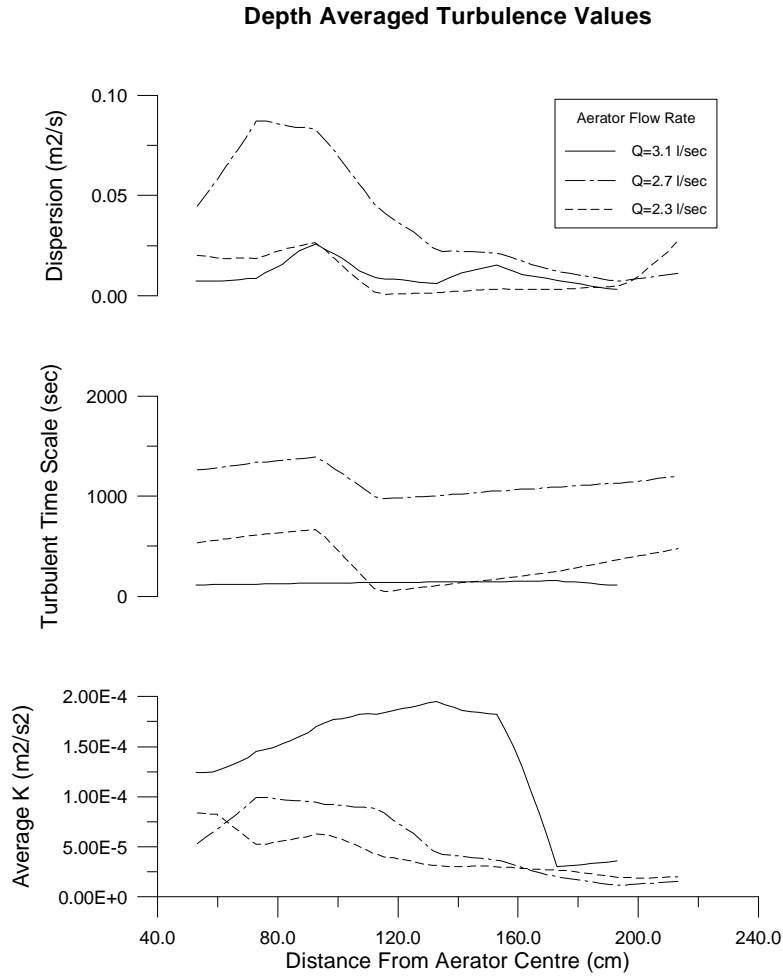


Figure 6: Depth-averaged turbulence values.

## TRACER STUDIES

### Basin modification for flow-through studies

In order to prepare the basin for tracer studies, the basin had to be adjusted from a still basin configuration, in which studies were performed on the aerators alone, to a flow-through configuration (Figure 7). In order to do this, two baffles were introduced to conduct the flow into and out of the basin. At the end of the outlet baffle section, a fixed weir was added that was 42 cm high from the floor of the basin. This inlet/outlet configuration was decided upon because of its potential to produce flow patterns that are not laterally uniform and at the same time to make use of the entire flow space and to minimize short-circuiting. This weir was used to control the height of the water in the basin. Beyond the weir a hole was cut in the side of the basin wall to allow water to drain out. Water was fed into the basin by a large hose that was attached to the city water supply. The flow rate was adjusted by a valve at the terminus of the

hose. Flow rate was measured by using a 25 liter bucket that was calibrated to the liter and with a stopwatch to time the flow duration. Three measurements were taken and timed prior to the start of the tracer run and averaged to determine the flow rate. The issue of flow rate changes due to pressure fluctuations in the distribution system was a concern. Flow measurements were taken after the completion of some runs and it was determined that, if flow rates changed at all, the changes were small and within the error of measurement.

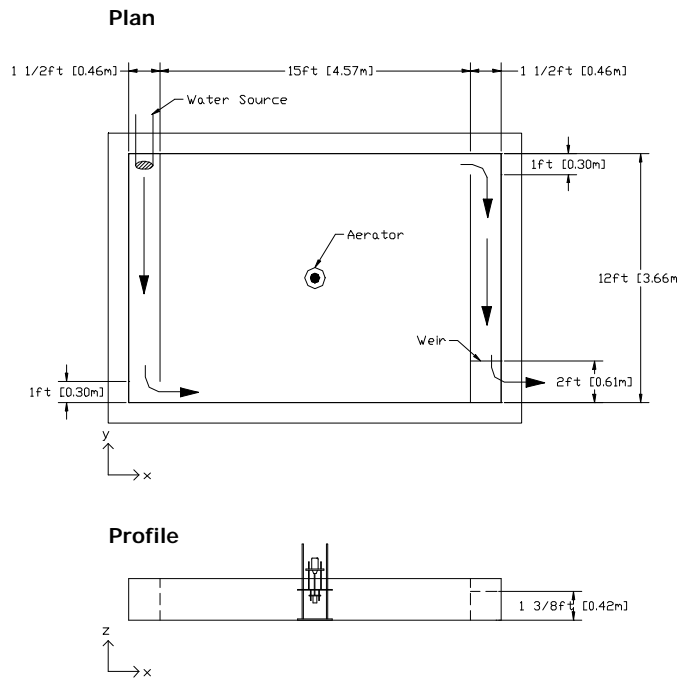


Figure 7: Modified basin for flow-through conditions.

### Tracer addition and sampling routine

The performance of the tracer studies was done with as much adherence to the NCASI procedures as was possible under the circumstances (NCASI, 1983). Flow rates through the basin were set to 2, 3, or 4 L/sec, because these flow rates produced hydraulic retention times that were reasonable for experimentation and were fast enough to induce turbulent flow in the basin. Flows in excess of 4 L/sec were very difficult to accurately measure.

It was generally found that the shape of the tracer C-curves changed appropriately with increases in flow rate and aerator power, (i.e. increased mixing produced more CSTR-like curves). Visual observations made of the basin while the tracer studies were performed seemed to corroborate these findings. The aerators had a very significant impact on the flow fields, drawing tracer to the center of the aerator almost immediately. The slow moving regions of the

tank tended to hold the tracer for longer periods of time, only gradually releasing the tracer into the faster moving flow path. Differences between various basin flow-through rates could not be easily determined by visual inspection. The recirculation of tracer was very much evident, with the majority of the tracer being discharged after the first pass of the outlet, leaving the remainder to circle around and be discharged at the second pass. By the time the third complete circulation was reached, the tank usually appeared to be completely mixed.

Some complications arose in the non-aerated runs, in that the lack of mixing often lead to streaks of dye that would stream through the outlet. Since the sampling was regular and samples were only taken at the prescribed time at the center of the outlet region, large amounts of dye could be missed entirely, or conversely, a streak could be captured, resulting in an unusually high concentration sample. The streaking of the dye was only observed at the time of the initial peak and was generally more pronounced in the slower moving, quiescent runs (i.e. 2 L/sec). This variation can be observed in the peaking in the runs without aeration.

### Parameter trends

Some interesting trends appeared in the analysis of the parameters derived from the tracer data collected. In the analysis of the effects of aerator power (measured as flow rate through the aerator) one can see interesting trends as seen in Figure 8. The peak concentration decreased with increasing aerator power; this was expected as mixing increased. Also, the mean and median times increased with an increase in aerator power. This phenomenon could be attributed to increased mixing in a system that would otherwise exhibit short-circuiting. An interesting observation is that the dispersion numbers and variance of the distribution dropped with an increase in aerator power, as did the Morrill index, which is also a measure of degree of mixing. This is difficult to explain but may have much to do with the recirculation zone and the periodic re-occurrence of tracer in the C-curve. These re-occurrences of tracer will have a significant effect on the variance, as they occur some time after the first peak has already passed. This could explain the high dispersion numbers exhibited in those tracer studies with no aeration

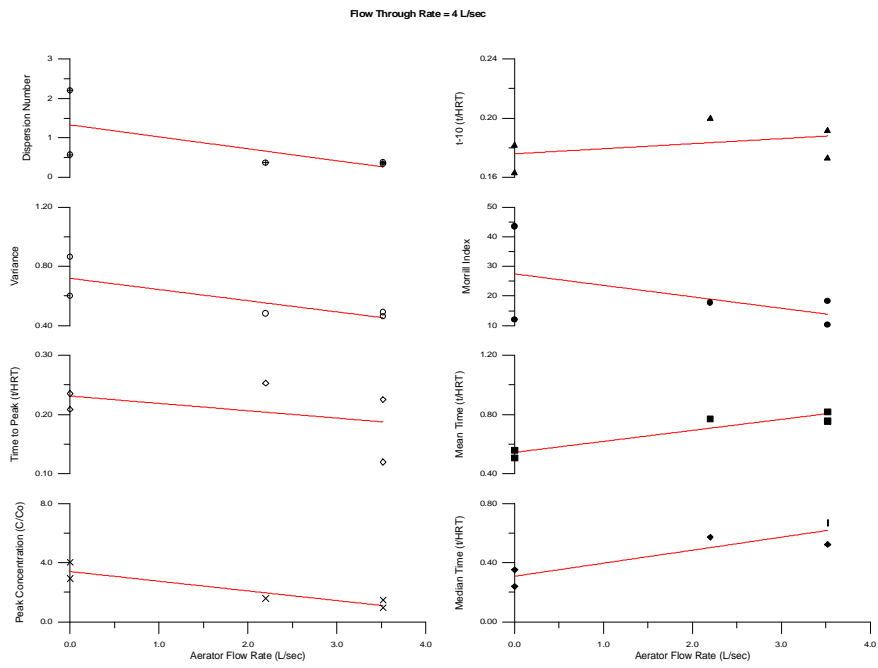


Figure 8: RTD parameters based on various aerator power settings.

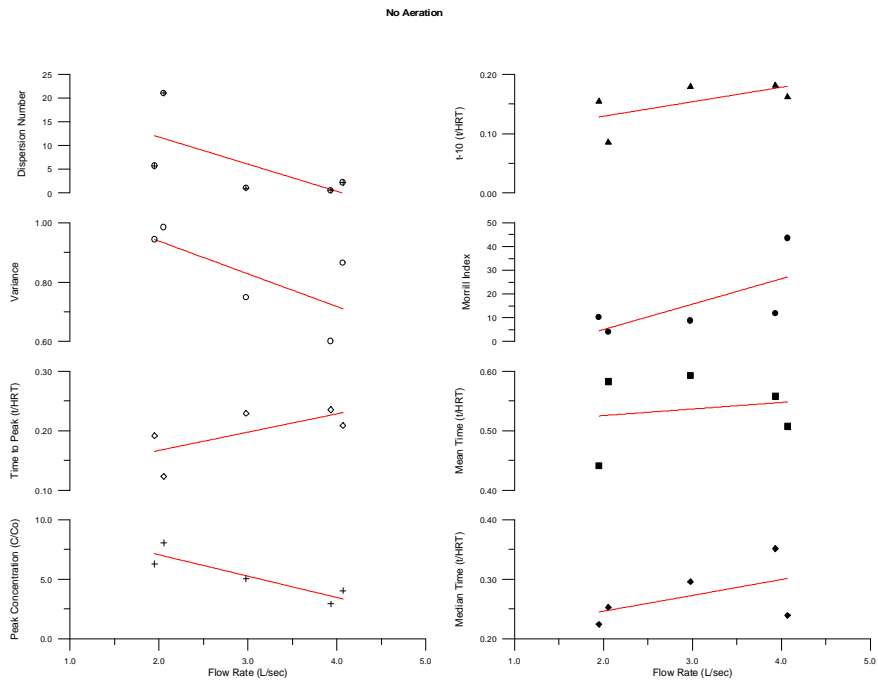


Figure 9: RTD parameters for various flow-through rates without aeration.

The effect of varying flow-through rate on the parameters illustrates some interesting trends shown in Figure 9. The peak concentration dropped with an increase in flow rate. This seems to be rational as an increase in the Reynolds number should result in an increase in turbulence at the

inlet and outlet regions. However the dispersion and variance parameters also decreased with an increase in flow rate, which seems to indicate a reduction in mixing. In direct contrast, the Morrill Index increased with an increase in flow rate.

## **FLUENT NAVIER-STOKES MODEL**

In order for the tracer model to be effective, it was necessary to know the flow patterns within the basin on a very detailed scale. A computational fluid dynamics model was employed to reproduce the fluid flow profiles exhibited in the previous section regarding tracer studies. The commercial CFD model FLUENT, installed on a PC was used to calculate the fluid flow patterns. FLUENT employs a finite-volume method for solving the fluid flow equations over structured meshes with a variety of turbulence models available.

### **Comparison of FLUENT to laboratory data**

In order to determine if the FLUENT model was producing accurate flow predictions, laboratory flow data were collected using the ADV to determine if the calculated flow fields could be considered valid. The data were collected at various points within the basin as illustrated in Figure 10 below, at points marked A through J. At each point, the velocity was sampled at 4 depths. The velocities were averaged and the result was considered to be the representative velocity at that point. Velocities were converted to U and V velocity components that corresponded to the FLUENT flow directions and compared to the velocities found in FLUENT grid solutions. Table 2 below shows the coordinates of each of the points with the distances being measured from the bottom left corner of the active basin at the inlet. The sampling points were primarily selected to lie on paths of highest velocity (A through G). The remainder of the sampling points (H through J) were added afterward to resolve uncertainties in the flow path.

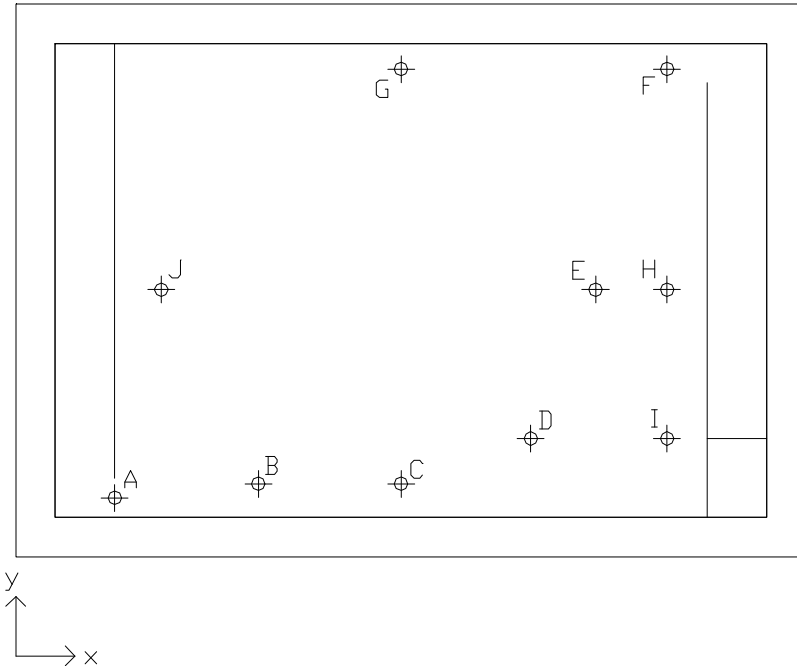


Figure 10: Velocity sampling points within basin.

Table 2: Velocity sampling points

<b>Sample Point</b>	<b>X(m)</b>	<b>Y(m)</b>
A:	0	0.15
B:	1.11	0.26
C:	2.21	0.26
D:	3.21	0.81
E:	3.71	1.76
F:	4.26	3.46
G:	2.21	3.46
H:	4.26	1.76
I:	4.26	0.61
J:	0.36	1.76

It was found that different mesh types produced reasonable results in terms of matching the flow, but the best results were obtained with a non-uniform mesh. The comparison was performed on the 2 L/sec model run with both uniform and non-uniform meshes at a resolution of 120x96 grid elements.

Table 3 below shows the values of the root mean square of the error between the predicted and the measured velocities, comparing grid shape. Three elements were compared, the velocities in the U direction, the velocities in the V direction and the velocity magnitude. Figure 11 below illustrates the associated errors with the change in grid shape for a mesh of 120x96.

Table 3: RMS error by mesh type

<b>Measurement</b>	<b>Root Mean Square Error (m/s)</b>	
	<b>Uniform Mesh</b>	<b>Non-Uniform Mesh</b>
U Velocity	0.00559	0.00505
V Velocity	0.00112	0.00073
Velocity Magnitude	0.00509	0.00468

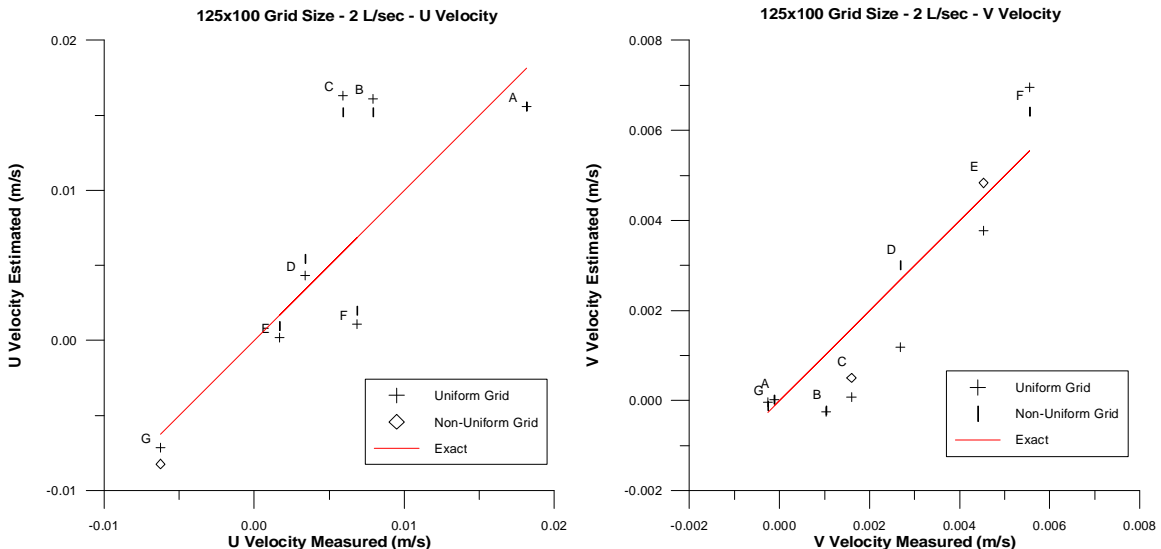


Figure 11: Fluent calibration – grid shape.

### Turbulence modeling and inlet configurations

Many parameters can be varied when modeling using CFD techniques. Two issues of concern were the inclusion or exclusion of turbulence modeling ( $k-\epsilon$  in this case) and the flow inlet boundary conditions. The modeling was performed with and without the  $k-\epsilon$  model and with a uniform velocity inlet and a parabolic inlet velocity boundary condition.

It was found that convergence could not be reached with the laminar flow modeling. Analysis of the residual histories indicated that the model seemed to approach convergence and then diverged to another flow condition and then oscillated about this solution.

Even though convergence was not reached with the laminar model, it was thought that perhaps the solution that the laminar flow model approached (but never reached) was a closer approximation to the measured velocities than that with turbulence modeling and proper convergence. Figure 12 below shows the various flow fields generated with either the laminar or turbulent models and with different inlet configurations. It can be seen that the flow fields are all generally similar with obvious differences observed at the inlets and in the shape of the recirculation patterns. The tighter circulation pattern observed for the parabolic inlet with laminar flow modeling (with two circulation zones) was of concern because it was difficult to ascertain from observation if the flow fields in the actual basin circulated with such a pattern. Comparison of the flow fields with additional data measured in the basin (points H, I and J) were used to examine this possibility. Table 4 below lists the RMS error values for the various flow components by turbulence model and inlet configuration. Figure 13 below shows the relative accuracy at these points, compared to laboratory ADV data.

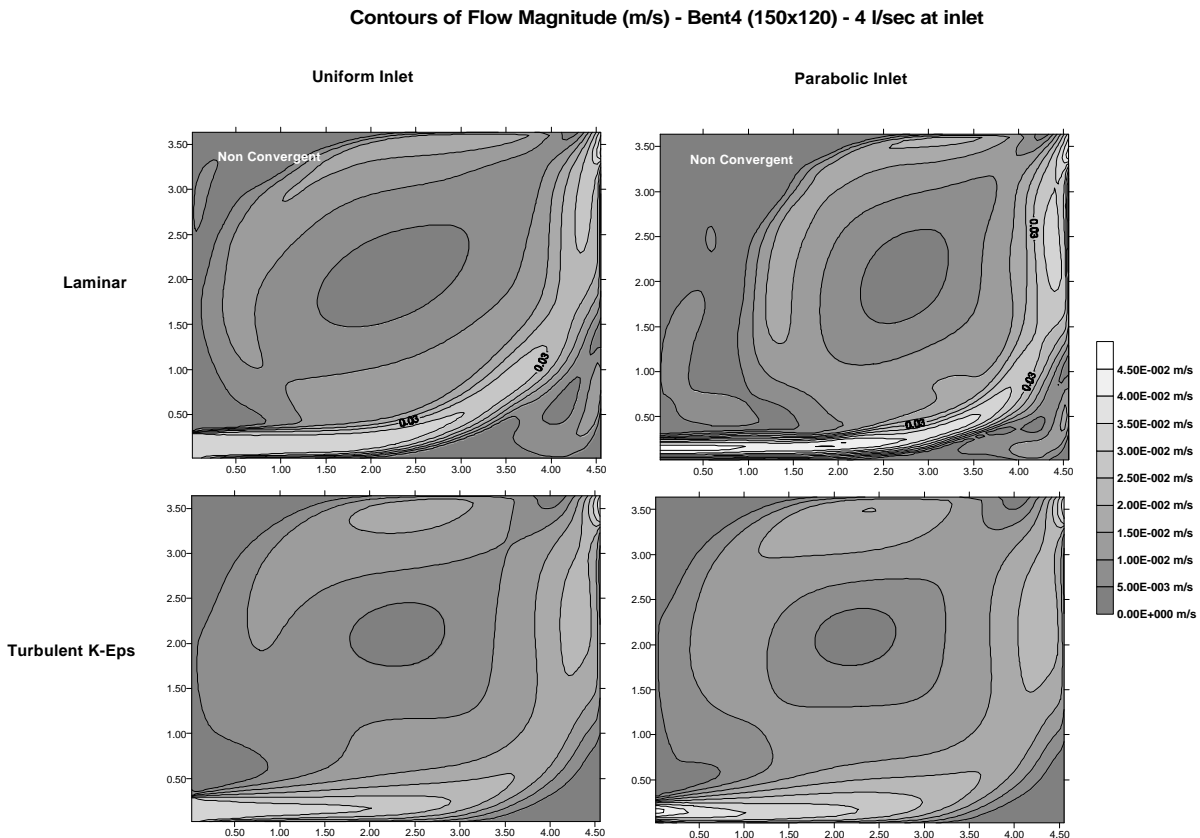


Figure 12: Velocity flow fields - comparison of turbulence and inlet configurations.

Table 4: RMS error by turbulence modeling and inlet configurations

Root Mean Square Error (m/s)				
	150x120 Bent4			
Measurement	Laminar, Uniform (non converge)	Turb, Para	Turb, Uniform	Laminar, Para (non converge)
U Velocity	0.0076	0.0054	0.0057	0.0095
V Velocity	0.0043	0.0036	0.0037	0.0073
Velocity Magnitude	0.0080	0.0063	0.0066	0.0103

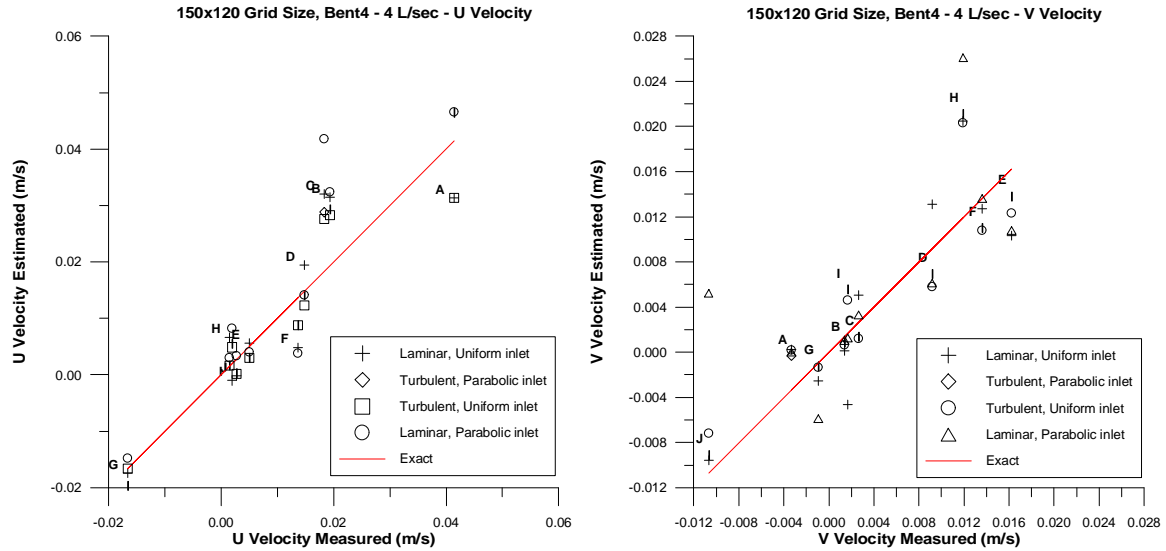


Figure 13: Flow calibration - comparison of turbulence and inlet configurations.

A review of the information for specific calibration points revealed some interesting aspects of the modeling. Samples taken at point A (at the inlet) showed that the inlet is more like a parabolic velocity profile than a uniform velocity profile, but that the best representation was somewhere in between.. Most likely, the flow profile was logarithmic in nature. The results also distinctly show that the parabolic inlet more accurately modeled the outlet as well (point F). It can also be seen that the turbulence modeling improved the overestimation of the velocities at points B and C, due to the dissipation of the momentum into turbulent structures. Also, the tight circulation observed with the laminar flow regime with a parabolic inlet was refuted with the observations at point J, where the V velocity in that case indicates flow in the opposite direction.

## CFD TRANSPORT MODEL

In order to calculate the RTD profile of the basin, it was necessary to incorporate a species transport model into the CFD modeling. The licensed version of the FLUENT modeling package that was employed for the Navier-Stokes equation modeling was not equipped with a species transport model. Therefore, it was necessary to develop a species transport model employing CFD techniques that could use the solutions provided by the FLUENT modeling to predict RTDs. The species transport code developed in this study was collectively named TRANSPORT. The model was developed using Visual Basic.

### RTD modeling

The modeling of the advection-dispersion scalar transport equations in conjunction with the flow fields developed using the FLUENT model allowed for the determination of the concentration profiles within the basin and for the generation of RTD profiles. The modeling was performed without consideration of the aerator effects and the inclusion of dispersion number values was applied globally to the solution space, not considering turbulent transportation of the conservative tracer.

It was found from visual inspection of the plots generated by the solute transport model that it seemed to be modeling with accuracy and the results seemed to match the results observed when the tracer studies themselves were performed on the basin. Of special interest was the location of the dead zones and the accumulation of dye at the top-left and bottom-right corners as well as in the center of the tank. These observed patterns were mimicked by the solute transport model. times for a model with a 4 L/s flow-through rate and a 100 mass unit addition of scalar across the inlet at time  $t = 0$ . Figure 14 below shows four snapshot times for a model with a 4 L/s flow through rate and a 100 mass unit addition of scalar across the inlet at time  $t = 0$ .

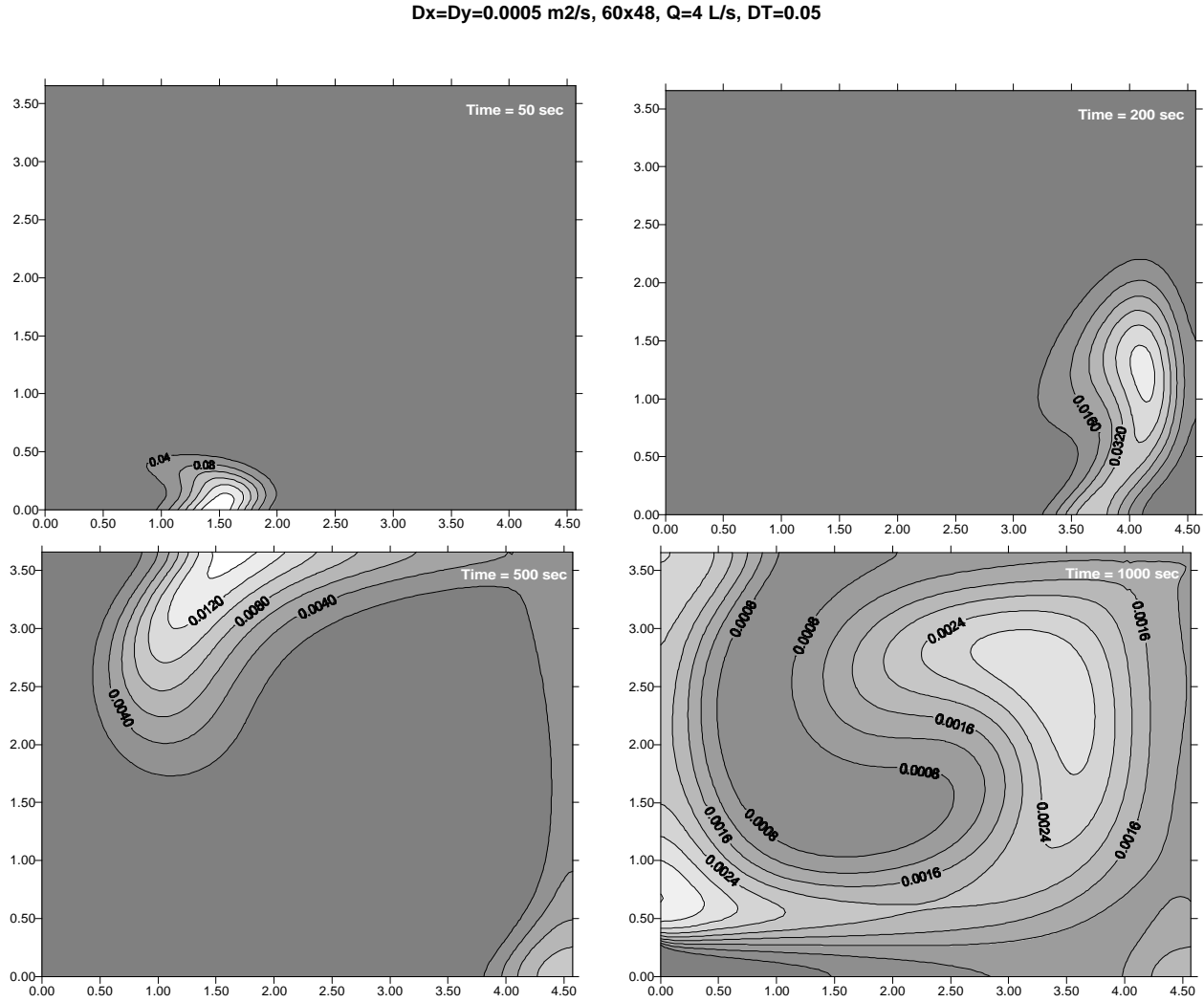


Figure 14: Sample solute transport time series – pulse tracer input.

## Continuity errors

It was discovered after examining the time series of the mass of the scalar in the basin and the corresponding outlet concentration-based RTD curves, that some mass was being lost during the runs. It was found that the mass that was added to the basin quickly decreased long before the tracer reached the outlet of the basin. Figure 15 below illustrates the sum total of mass in the solution space and the concentration at the outlet time series for the same run illustrated previously in Figure 14. It can be seen that the mass decreased from the initial value of 100 to about 63 after the first few iterations and this loss did not correspond to any concentration at the outlet. It is believed this initial dramatic drop was due to diffusion of mass out of the basin through the inlet. However, it was seen that there was a slow decrease in mass in the basin until about 250 seconds, when the scalar cloud actually reached the outlet and started to exit the

system normally. This drop was believed to be caused by lack of continuity in the flow fields employed in calculation.

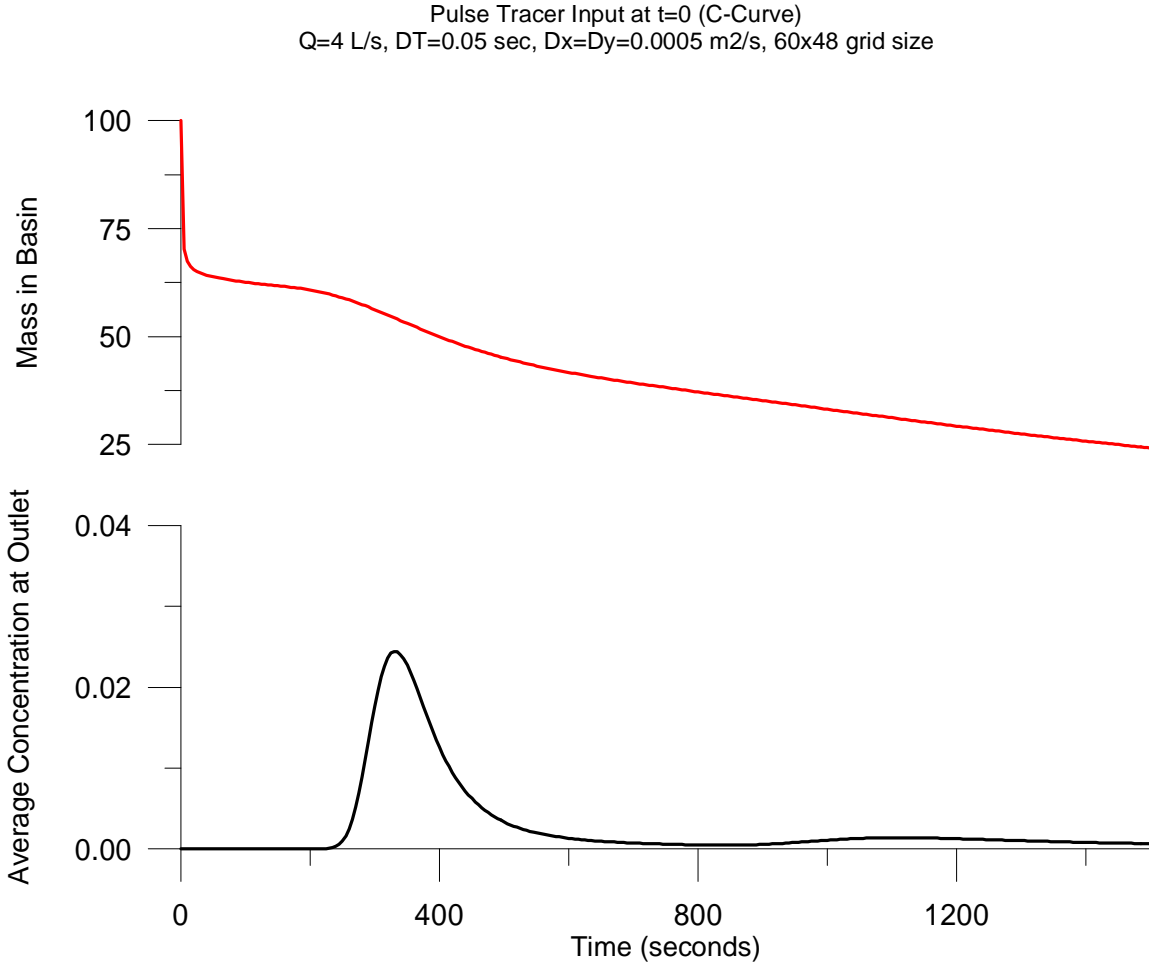


Figure 15: Mass and outlet concentration time series – pulse tracer input.

In an attempt to assess these issues, two steps were taken. As a first step, a continuous input of tracer was assumed instead of a pulse input of tracer while modeling, thus reducing any negative flux of the tracer out of the basin at the inlet. The second step involved an analysis of the FLUENT flow field being employed to determine whether continuity was satisfied over the whole space.

The switch from a pulse injection to a continuous feed of tracer was accomplished by setting the concentration at the inlet boundary to a specified value (100 concentration units). This allowed both advection and dispersion of the tracer into the basin, and conversely limited the amount of tracer dispersing out the inlet (because the tracer concentration at the inlet would be higher than that just within the basin). Figure 16 and 17 below illustrate the snapshots of the concentration profiles and the mass and concentration time series respectively, for the continuous

tracer input configuration. It can be seen by examining the outlet concentration time series in Figure 17 that mass was not conserved. With an inlet concentration of 100 units as specified earlier, one would expect the final outlet concentration to be 100 also. This was not the case and clearly mass was being lost.

**Dx=Dy=0.0005 m<sup>2</sup>/s, 60x48, Q=4 L/s, DT=0.05**

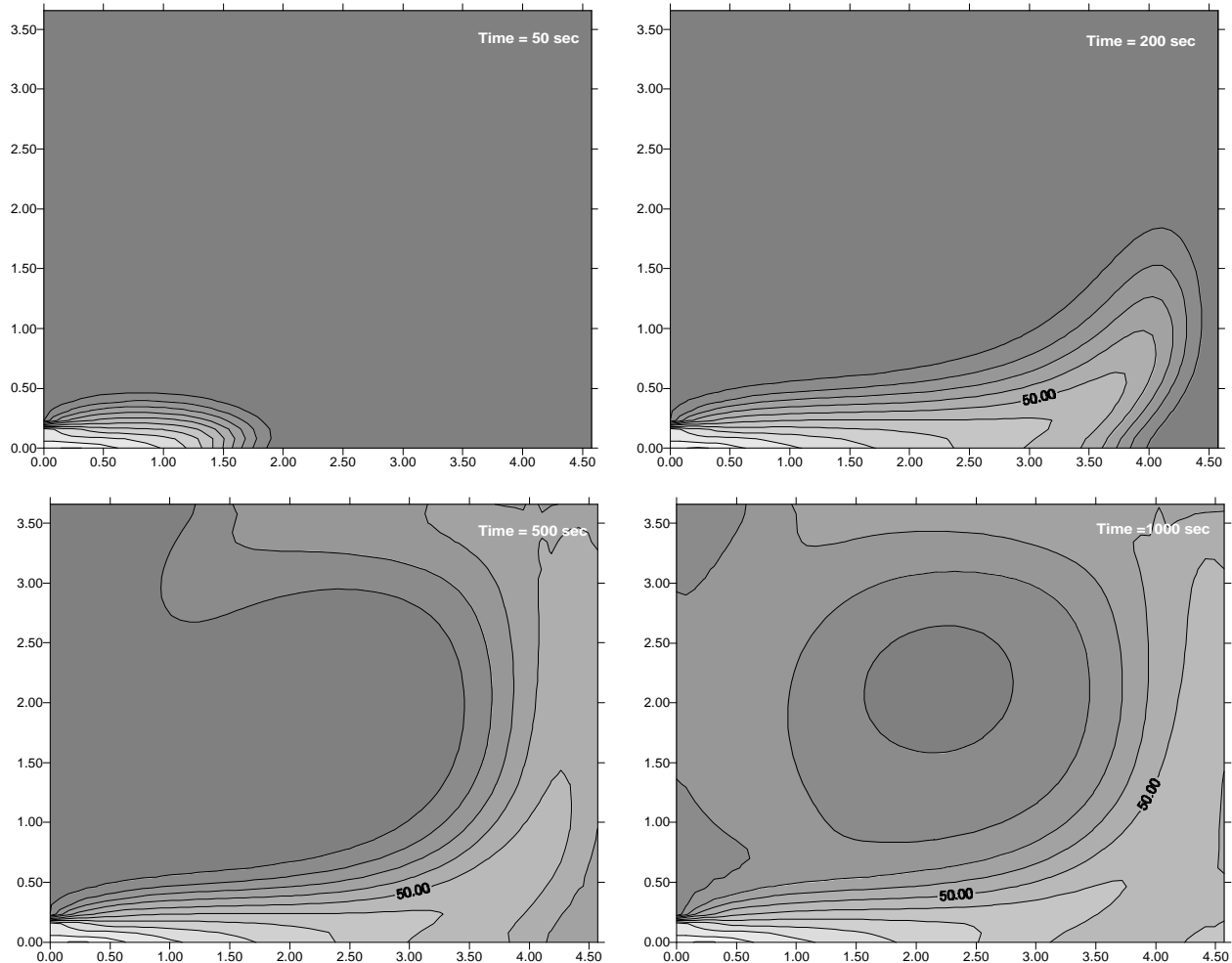


Figure 16: Sample solute transport time series – continuous tracer input.

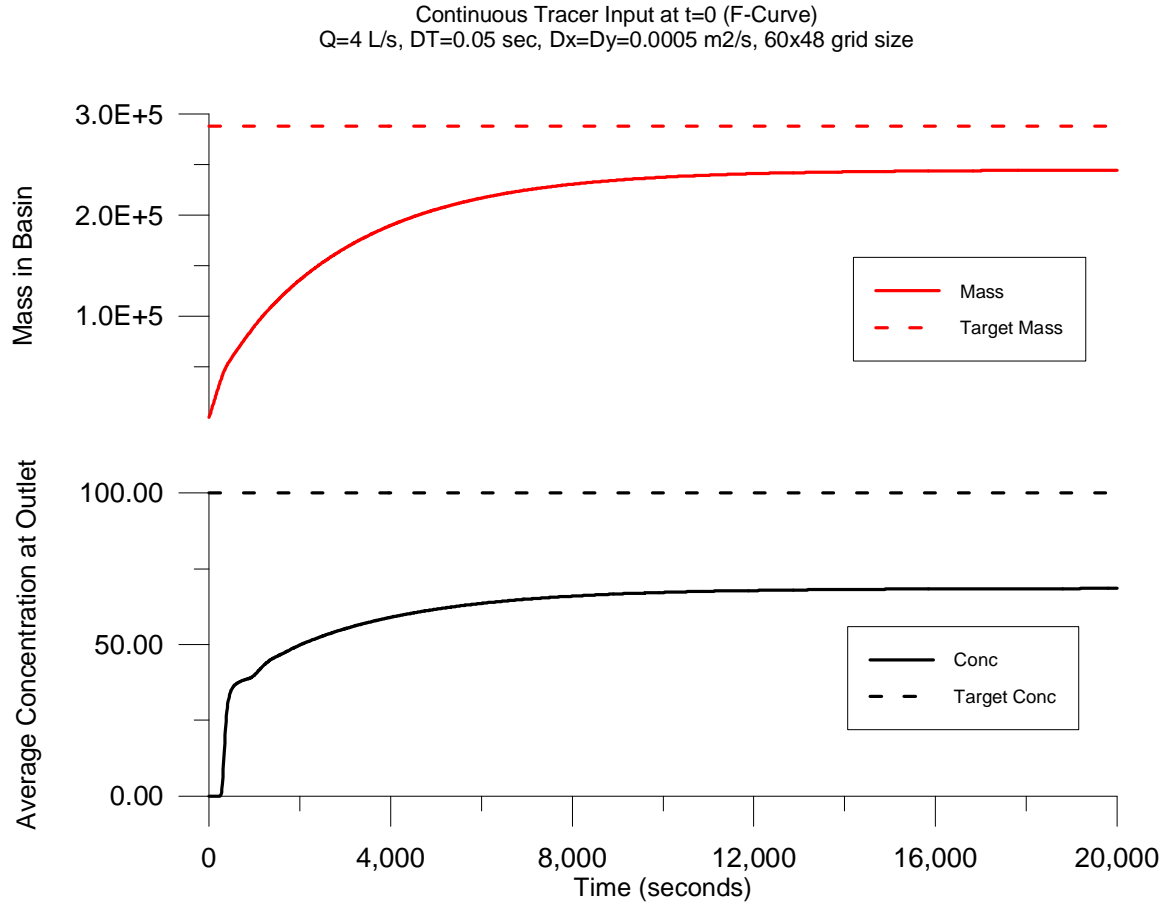


Figure 17: Mass and outlet concentration time series – continuous tracer input.

For a further explanation of the mass errors associated with the RTD data, the flow field itself was looked to for errors in flow continuity. The basin flow field was analyzed using the same routine used to analyze the still basin profiles for continuity as described previously. This routine was modified slightly in its output to produce a surface map of the magnitude of the continuity error, normalized to the magnitude of the local velocity gradient.

If continuity had been satisfied, then the plot would produce a surface of magnitude zero over the entire flow space. The worst local continuity error can be unity. The plot of continuity error over the solution space used in the RTD calculations is shown in Figure 18 below. It can be seen that the majority of the space exhibited good continuity satisfaction, but several areas violated the continuity criteria quite seriously, especially near the boundaries. It was believed that this continuity error was associated with the lost mass exhibited in the RTD routines. These errors were likely caused by the transformation routine that converted the non-uniform mesh to a uniform mesh for the tracer transport modeling.

150x120 - Turb, Para - Bent 4: Mapped to 60x48 Uniform

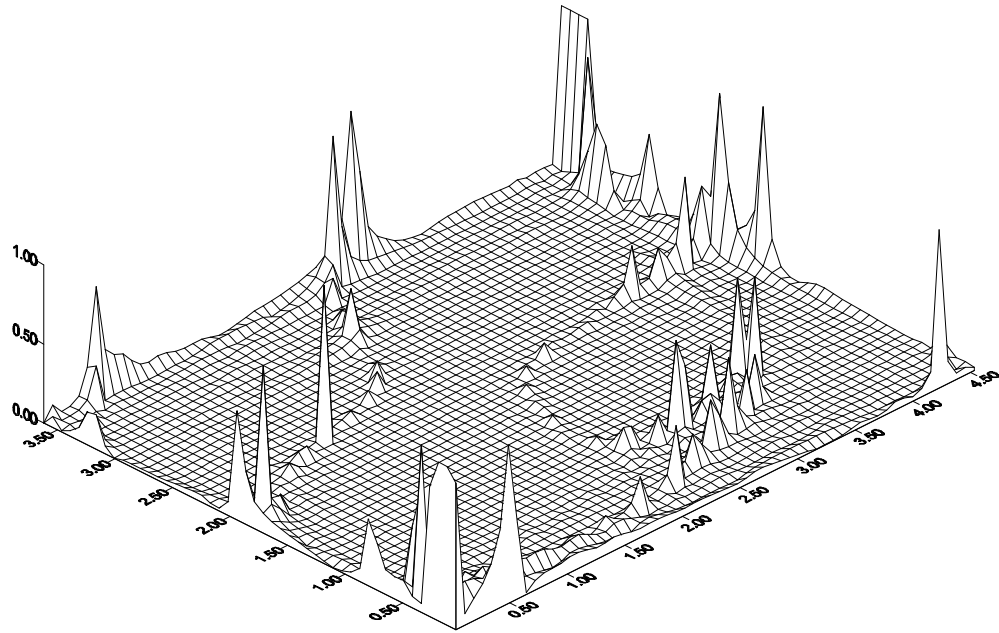


Figure 18: Normalized continuity error map

### Matching laboratory RTD profiles

Although issues have been presented regarding the evident loss of mass either by diffusion through the inlet or due to continuity errors in the flow fields, the RTD profiles generated by CFD can still be of value by considering the shape of the profiles in comparison to the laboratory tracer data discussed earlier. It was found that when the laboratory tracer studies and the generated RTD profiles were normalized for total mass for the first two hydraulic retention times, the profiles matched reasonably well. Figure 18 shows the excellent match in RTD shape between the laboratory data and the model results for 4 L/sec and no aeration. The model even captured the recirculation period between 0.5 and 1.0 retention times, something that an axial dispersion model is incapable of doing. Additionally, the timing of the tracer appearance at the outlet, the time to peak and the time to recirculation are reproduced with satisfactory accuracy.

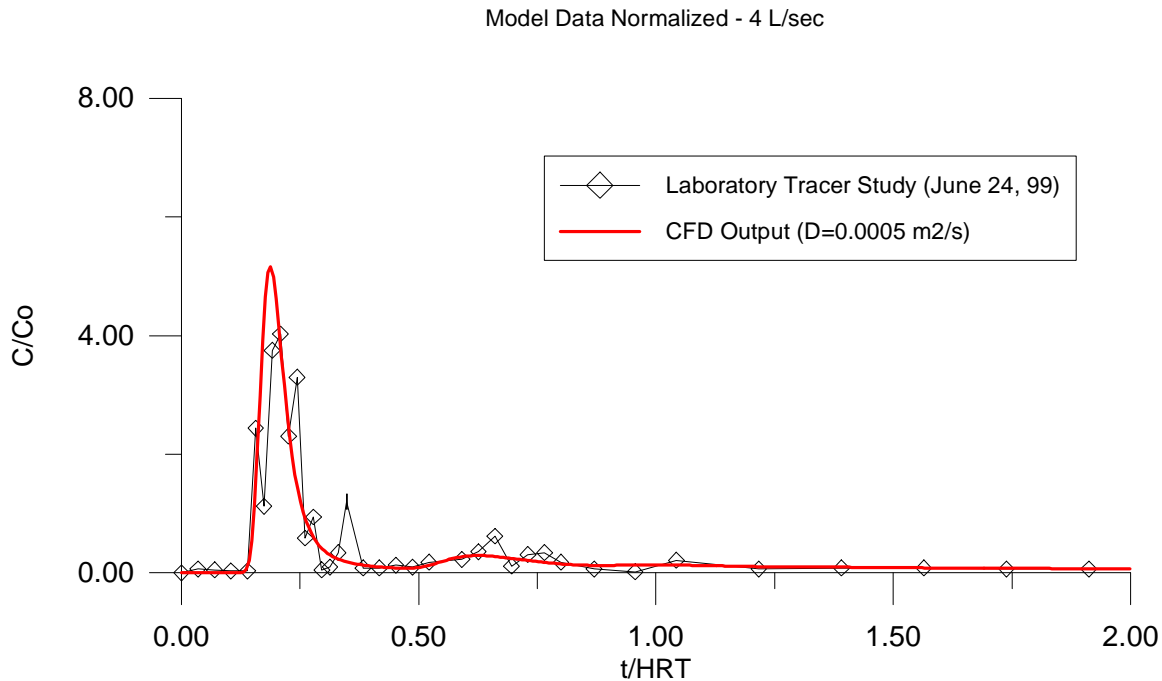


Figure 19: Comparison of model and laboratory C-curves.

## MANAGEMENT APPLICATIONS

The development of computer-based simulation models for aerated stabilization basin (ASB) secondary wastewater treatment systems is currently limited by difficulties in describing the hydraulic characteristics of these systems. This objective of the present study was to determine whether computational fluid dynamics (CFD) techniques could be useful for modelling the hydraulics of ASBs. In order to assess the CFD approach, a well defined pilot-sized tank was used to collect velocity and turbulence data and to generate residence time distribution information for simulation with CFD models.

The results of the study indicated that the CFD techniques offer considerable promise for modelling the hydraulics of ASB systems, although further work is required to develop CFD models that incorporate the effects of the surface mechanical aerators that are commonly used in ASBs. Ultimately, this approach may allow the hydraulics of ASBs to be simulated without the need for the detailed experimental surveys and tracer studies that are currently required. Properly calibrated and verified CFD models could then be used to simulate the effects of such physical parameters as aerator placement, aeration power input and basin geometry on the resulting hydraulic characteristics of full-scale ASBs.

## CONCLUSIONS AND RECOMMENDATIONS

### Conclusions

It was the objective of this study to examine the potential of modeling ASBs with computational fluid dynamics, using data generated with a laboratory scale apparatus. This analysis was primarily investigative, examining a variety of analytical and modeling approaches. The project was successful in that the apparatus was constructed and tested in a variety of ways, including still basin analysis for aerator impacts, tracer studies on a modified flow-through basin with a variety of flow rates and aeration levels, and reasonably successful fluid flow modeling and species transport.

The construction of the aerator and the basin was completed with a good degree of care to ensure a range of flow rates and mixing that ensured reasonable similarity with actual ASBs. True similarity was difficult to accomplish due to the splashing and other scale issues, but the range of flow rates of the scale apparatus seemed to produce a good variety of mixing conditions.

The trends presented regarding turbulence profiles in the still basin analysis were inconclusive and the difficulty in resolving flow continuity with the vertical plane sampling technique presented analytical difficulties. However, the analysis did provide insight into the extent of the complexity of the flow imparted by aeration. Additionally, it was found that the method employed to approximate the dispersion number profiles must be refined and tested, so that some mixing characteristics might be used in a CFD mixing model.

The FLUENT flow modeling was a success in that it predicted the velocity measurements in the basin with a good degree of accuracy. The variety of techniques employed to refine the solution were reasonably successful, with a turbulent model with a parabolic inlet profile providing the most accurate results. The modeling might have benefited from the inclusion of more realistic governing equations, namely equations that accounted for the shear stress from the basin floor.

The manufactured CFD code for species transport was also fairly successful. The model was developed successfully with an accurate replication of the analytical advection-dispersion cases. However, when combined with the modified flow results acquired from FLUENT, the results suffered from mass conservation losses. It is suspected that the mass losses are likely due to the continuity errors associated with the flow field and/or a steady-state dispersion out of the inlet. These problems could be addressed by converting the flow fields to a structured grid with a more complex routine and by coding in a strict flux restriction at the model inlet. The reproduction of

the shape of the RTD from the tracer studies without aeration was quite good, although a mass correction was required to make such a comparison.

## **Recommendations**

The following list outlines some of the recommendations for further study:

1. It is recommended that more data be collected in the still basin study. With enough velocity profiles it might be possible to elucidate trends in turbulent time scale or dispersion numbers as related to the flow through the aerator and the distance of sampling point from the aerator.
2. The resolution flow continuity in the still basin data is also an issue of great importance. It could be worth investigating whether continuity can be resolved at all using the ADV within the basin, with a series of time-averaged point data. A detailed examination of a small area within the basin in three dimensions (rather than two) may yield more fruitful results.
3. The still basin aeration analysis might also benefit from examining the flow fields introduced by an aerator close to a wall boundary. If it could be found that the profiles of turbulent diffusion could be mapped to a 2D CFD model then knowledge of the impacts of boundaries would be valuable.
4. The tracer studies could be improved upon primarily through further data collection. However, the mixing impacts of other factors such as a change in water depth, the introduction of baffles or the placement of the aerator would also be of interest.
5. The FLUENT modeling could be improved upon by attempting to incorporate the shear stress at the bottom of the basin either through the introduction of the stress to the two-dimensional equations or through three-dimensional flow modeling.

The CFD scalar transport model could be improved upon by examining the lack of mass conservation associated with the model and determining which phenomena are the causes. The model could also be improved by including turbulent transport into the dispersion model and including a technique to include space-variable dispersion into the model that could approximate the influence of aerators.

## **REFERENCES**

AQUA-AEROBIC SYSTEMS, INC. Bulletin No. 950F 2/98 (1998)

FISHER, HUGO B.; LIST, E. JOHN; KOH, ROBERT C. Y.; IMBERGER, JORG; BROOKS, NORMAN H.; (1979), Mixing in Inland and Coastal Waters, *Academic Press*

JENKINSON, R.W.; (2000), Analysis of Laboratory Scale Aerated Basin Using Computational Techniques, M.A.Sc. Thesis, Department of Civil Engineering, The University of British Columbia.

NAMECHE, TH; VASEL, J. L.; (1998) Hydrodynamic Studies and Modelization for Aerated Lagoons and Waste Stabilization Ponds, *Wat. Research*, **12** (10) pp.3039-3045

NCASI; (1971) A study of mixing characteristics of Aerated Stabilization Basins, *NCASI Tech. Bull.*, No. 245

NCASI; (1983) A review of procedures for conducting conservative tracer studies in the hydraulic characterization of effluent treatment basins, *NCASI Tech. Bull.*, No. 408